

Chromosomal Dynamics at the *Shh* Locus: Limb Bud-Specific Differential Regulation of Competence and Active Transcription

Takanori Amano,¹ Tomoko Sagai,¹ Hideyuki Tanabe,² Yoichi Mizushima,¹ Hiromi Nakazawa,¹ and Toshihiko Shiroishi^{1,*}¹Mammalian Genetics Laboratory, Genetic Strains Research Center, National Institute of Genetics, 1111 Yata, Mishima, Shizuoka 411-8540, Japan²Biosystems Science, School of Advanced Sciences, The Graduate University for Advanced Studies, Shonan Village, Hayama, Kanagawa 240-0193, Japan*Correspondence: tshiroishi@lab.nig.ac.jp

DOI 10.1016/j.devcel.2008.11.011

SUMMARY

The expression of Sonic hedgehog (*Shh*) in mouse limb buds is regulated by a long-range enhancer 1 Mb upstream of the *Shh* promoter. We used 3D-FISH and chromosome conformation capture assays to track changes at the *Shh* locus and found that long-range promoter-enhancer interactions are specific to limb bud tissues competent to express *Shh*. However, the *Shh* locus loops out from its chromosome territory only in the posterior limb bud (zone of polarizing activity or ZPA), where *Shh* expression is active. Notably, while *Shh* mRNA is detected throughout the ZPA, enhancer-promoter interactions and looping out were only observed in small fractions of ZPA cells. In situ detection of nascent *Shh* transcripts and unstable *EGFP* reporters revealed that active *Shh* transcription is likewise only seen in a small fraction of ZPA cells. These results suggest that chromosome conformation dynamics at the *Shh* locus allow transient pulses of *Shh* transcription.

INTRODUCTION

Recent studies indicate that transcriptional activity is correlated with changes in higher-order chromatin structure in higher metazoans (Foster and Bridger, 2005; Cremer et al., 2006; Fraser and Bickmore, 2007; Lanctôt et al., 2007). In the interphase nucleus, individual chromosomes form structural domains known as chromosome territories (CTs). Both the nuclear position of chromosomes and the location of gene loci relative to CTs are important for regulation of gene expression during development and differentiation. For example, chromatin decondensation is observed in the transcriptionally active *Hoxb* gene cluster, with transcribed genes looping out from the CT (Chambeyron and Bickmore, 2004). This loop formation occurs in a tissue- and stage-specific manner and is coupled with colinear expression of *Hoxb* genes in mouse embryos (Chambeyron et al., 2005). In contrast, *Hoxd* genes do not loop out from the CT in mouse limb buds when they are actively transcribed (Morey et al.,

2007), suggesting that gene relocation is not a general phenomenon among *Hox* clusters.

It has also been reported that many genes have long-range enhancers that sometimes map beyond hundreds of kilobases away from the promoter (Kleinjan and van Heyningen, 2005; West and Fraser, 2005; Li et al., 2006). In the case of β -globin genes, long-range enhancers within the locus control region (LCR) interact with target genes by looping out of the intervening chromosomal segment (Carter et al., 2002; Tolhuis et al., 2002). Moreover, interchromosomal contact between coding regions and LCRs occurs in actively transcribed genes (Spilianakis et al., 2005; Ling et al., 2006). Thus, dynamic changes in chromosome conformation are crucial for proper gene expression at many loci. However, why organisms employ such a complex, large-scale mechanism to regulate gene expression remains unknown.

Sonic hedgehog (*Shh*) encodes a signaling protein that plays pivotal roles in many processes during vertebrate development (Riddle et al., 1993; McMahon et al., 2003). In the developing limb bud, *Shh* is expressed exclusively in the posterior mesenchyme, a region known as the zone of polarizing activity (ZPA). The ZPA establishes a concentration gradient of secreted *Shh* protein along the anteroposterior axis in the limb bud, and digit identity has been linked to the *Shh* concentration (Tickle, 1981; Riddle et al., 1993). Thus, initiating and maintaining appropriate *Shh* expression levels in the ZPA is critical for normal digit morphogenesis.

Evolutionarily conserved elements near the *Shh* coding region are known to act as enhancers for floor plate- and notochord-specific gene expression (Epstein et al., 1999). A highly conserved sequence named mammal fish conserved sequence 1 (MFCS1) is found in intron 5 of the *Lmbr1* locus (Figure 1A; Lettice et al., 2003; Sagai et al., 2004), approximately 1 Mb upstream of the *Shh* transcription start site (TSS). Many lines of evidence indicate that MFCS1 contains a limb bud-specific *Shh* enhancer (Lettice et al., 2003; Sagai et al., 2005; Masuya et al., 2007), including our previous report showing that deletion of MFCS1 abolishes *Shh* expression specifically in the limb buds and consequently disrupts formation of distal skeletal elements of the limb (Sagai et al., 2005). Although this long-range enhancer clearly mediates limb bud-specific *Shh* gene expression, little is known about the possible molecular basis of this regulation.

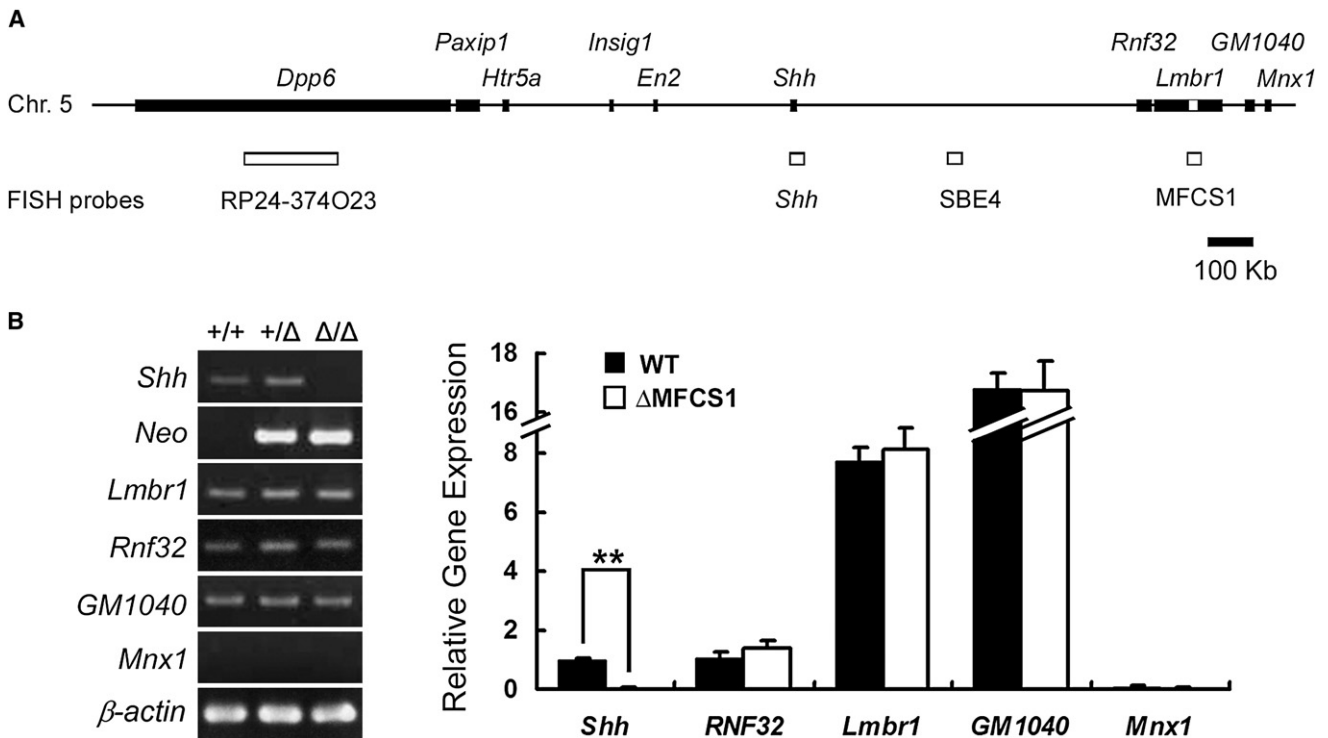


Figure 1. MFCS1 Contains an Enhancer that Specifically Regulates *Shh* Expression in Mouse Limb Buds

(A) Schematic diagram of the genomic region around the *Shh* locus on mouse chromosome 5. Limb-specific long-range enhancer MFCS1 is located in the *Lmbr1* intron (open box). Open boxes under the genomic region depict probes used for 3D-FISH experiments.

(B) Expression profiles of genes linked to *Shh* by RT-PCR. mRNA was prepared from forelimb buds of wild-type, heterozygous (+/Δ), and homozygous (Δ/Δ) E10.5 littermates generated from ΔMFCS1 heterozygous intercrosses. The right-hand graph shows the results of real-time PCR analysis of mRNA prepared from forelimb buds of wild-type (black bars) and ΔMFCS1 homozygous (open bars) embryos. Expression levels shown are mean values obtained from three independent PCR reactions and are normalized by β -actin expression levels. The expression level of *Shh* in wild-type limb buds was set as 1. Error bars represent standard deviations (SD) obtained from the experiments performed in triplicate. Double asterisks show significant differences, as evaluated by Welch's t test ($p < 0.01$).

Conditional loss of the *Hoxa* and *Hoxd* gene clusters has been shown to downregulate *Shh* expression in the mouse limb bud (Kmita et al., 2005), whereas the overexpression of *Hoxd* genes can induce ectopic *Shh* expression at the anterior margin of the limb bud (Knezevic et al., 1997; Zakany et al., 2004). Moreover, Hoxd10 and Hoxd13 proteins can bind directly to the MFCS1 enhancer (Capellini et al., 2006). These data suggest that the *Hoxd* genes are necessary and sufficient to induce *Shh* in limb buds. However, the *Hoxd* expression domain in the mouse limb bud is broader than the ZPA; thus, additional regulatory mechanisms must help to establish the spatiotemporal expression pattern of *Shh* in the developing limb bud. It is possible that tissue- and stage-specific modifications of chromosome conformation around the *Shh* locus play a role in this process (Sagai et al., 2005).

Here, we examine the dynamics of chromosome conformational changes in the nuclei of developing limb bud cells by visualizing the physical interaction between the MFCS1 enhancer and the *Shh* coding region via three-dimensional (3D)-FISH and chromosome conformation capture (3C) assays. We show that long-range interactions between the *Shh* promoter and the MFCS1 enhancer occur in both the anterior and posterior limb buds, reflecting the transcriptional competence of *Shh*. In contrast, looping out of the *Shh* locus from the CT occurs only in

the ZPA of the posterior limb bud, which actively expresses *Shh*. Interestingly, the enhancer-promoter interaction and the looping out from the CT were observed in only a small fraction of *Shh*-expressing cells in the ZPA. The expression patterns of *Shh* precursor-mRNA and unstable *EGFP* inserted in the *Shh* locus suggest that the transitional chromosome conformation of the *Shh* locus allows pulses of *Shh* transcription. Our data support a model in which fluctuating chromosome conformation leads to intermittent *Shh* expression in ZPA cells.

RESULTS

MFCS1 Regulates *Shh* Expression Exclusively in Developing Mouse Limb Buds

The 1 Mb genomic region spanning *Shh* to MFCS1 is extremely gene poor, and only four genes, *Mnx1*, *GM1040*, *Lmbr1*, and *RNF32* are currently mapped (Figure 1A). In the limb bud, *Shh* is expressed exclusively in the ZPA, whereas *Mnx1*, *Lmbr1*, and *RNF32* expression is not posteriorly localized. Although the elimination of MFCS1 ablates *Shh* expression in the mouse limb bud, it is not known whether MFCS1 also controls the expression of any other genes around itself. To test for other possible interactions, we examined the expression of *Mnx1*, *GM1040*, *Lmbr1*, and *RNF32* by real-time RT-PCR using limb

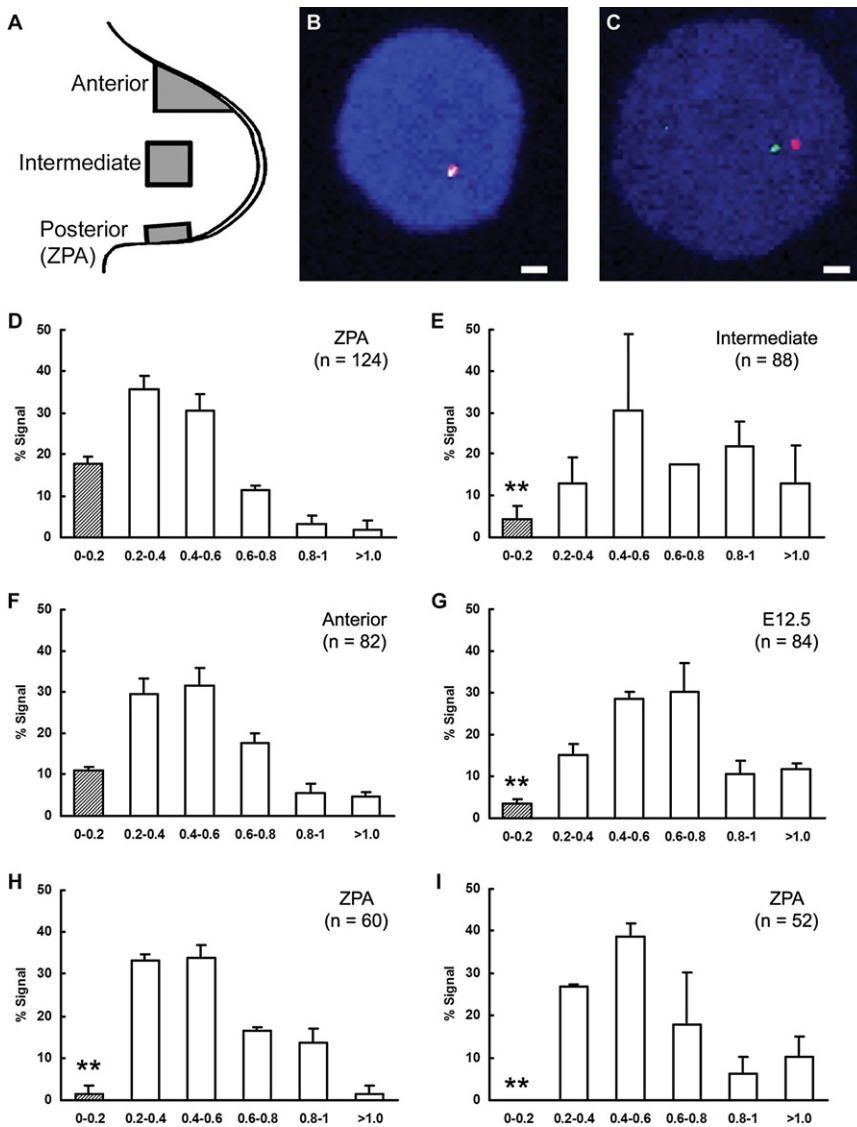


Figure 2. Physical Distance between MFCS1 and the *Shh* Coding Region in Limb Bud Cells

(A) Schematic diagram of forelimb bud of an E10.5 mouse embryo. The three shaded regions represent the anterior, intermediate, and posterior (ZPA) regions of the limb bud that were used in this study. Examples of colocalized hybridization signals (B) and separated signals (C) in confocal sections of the ZPA cells. Nuclei were stained blue with TOPRO-3. White bars, 1 μ m.

(D–G) Frequency distributions of the distance between MFCS1 and the *Shh* coding region. The frequencies were calculated for every 0.2 μ m distance interval. Single cell suspensions were prepared from the posterior limb bud at E10.5 (D), the intermediate region at E10.5 (E), the anterior edge at E10.5 (F) and the posterior third of the limb bud at E12.5 (G). The frequency distributions of the distance between SBE4 and *Shh* (H) and between MFCS1 and SBE4 (I) in ZPA cells. Shaded column indicates a fraction of colocalized signals (0–0.2 μ m). The chi-square test was used for evaluation of significant differences between the frequencies of the colocalized signals in the ZPA and each of other tissues (** $p < 0.01$). Number (n) of loci observed in this experiment is shown. Error bars represent the standard deviations (SD) obtained from two independent experiments.

the physical distance between MFCS1 and the *Shh* coding region was calculated. MFCS1 and *Shh* signals colocalized in some nuclei (Figure 2B) but were separate in others (Figure 2C). Frequency distribution patterns of the physical distance between MFCS1 and *Shh* were obtained for each of the three limb bud regions (Figures 2D–2F). In the posterior, ZPA-containing region, 18% of the MFCS1 signal was in close proximity to the *Shh* signal (<0.2 μ m; Figure 2D), with

buds from E10.5 MFCS1 knockout (Δ MFCS1) embryos. We found that while *Shh* is downregulated, *GM1040*, *Lmbr1*, and *RNF32* remain at wild-type levels (Figure 1B) and *Mnx1* is absent in both wild-type and mutant limb buds. Thus, MFCS1 appears to function specifically as a long-range enhancer for *Shh*.

Spatiotemporal Changes in the Physical Distance between MFCS1 and the *Shh* Coding Region

To analyze the changes in chromosomal conformation around the *Shh* locus during limb development, we performed 3D-FISH analysis using *Shh* and MFCS1 probes on three-dimensionally preserved cell nuclei prepared from the developing limb buds of wild-type E10.5 mouse embryos. Limb buds were dissected into three regions along the anteroposterior axis, and then single cell suspensions were prepared separately from each limb bud region (Figure 2A). The posterior mesenchymal portion containing the *Shh*-expressing ZPA was excised with care to minimize contamination by other mesenchymal cells. After capturing 3D images of the two fluorescent signals,

the mean distance at $0.39 \pm 0.23 \mu$ m (Table 1). In contrast, in the intermediate limb bud, the frequency of colocalized signals (4%) was greatly reduced ($p < 0.01$, chi-square test), and the overall frequencies of separated signals were elevated as compared to those for the posterior limb bud ($p < 0.01$, Kolmogorov-Smirnov test; Figure 2E), with the mean distance at $0.68 \pm 0.38 \mu$ m (Table 1). Unexpectedly, many colocalized signals were observed in cells prepared from the anterior limb bud, where *Shh* is not expressed under normal conditions. The overall frequency distribution pattern of the MFCS1-*Shh* distance in the anterior limb bud cells resembled that in the posterior limb bud cells ($p = 0.179$, Kolmogorov-Smirnov test), although the frequency of colocalized signals tended to be lower (11%) than that observed in the latter cells ($p = 0.027$, chi-square test; Figure 2F). Since the anterior limb bud, unlike the intermediate regions of the limb bud that lack MFCS1-*Shh* interactions, does sometimes activate *Shh* expression in certain mutants (see Discussion below), it would seem that the MFCS1-*Shh* interaction may reflect transcriptional competence.

Table 1. Mean Distances between Two FISH Signals

Sample Type	Tissue	Probe Pair	Mean Distance \pm SD
Cell suspension	ZPA	<i>Shh</i> /MFCS1	0.39 \pm 0.23
	Intermediate	<i>Shh</i> /MFCS1	0.68 \pm 0.38
	Anterior	<i>Shh</i> /MFCS1	0.50 \pm 0.36
	E12.5 posterior	<i>Shh</i> /MFCS1	0.64 \pm 0.29
	ZPA	<i>Shh</i> /SBE4	0.52 \pm 0.26
	ZPA	MFCS1/SBE4	0.56 \pm 0.25
Section	ZPA	1 Mb control pair	0.86 \pm 0.40
	ZPA	<i>Shh</i> RNA/ <i>Shh</i>	0.19 \pm 0.10
	ZPA	<i>Shh</i> RNA/MFCS1	0.21 \pm 0.12
	ZPA	<i>Shh</i> RNA/control BAC	0.55 \pm 0.25
	ZPA	<i>Shh</i> /MFCS1	0.45 \pm 0.21
	Δ MFCS1	<i>Shh</i> /MFCS1	0.43 \pm 0.22

The mean distances between green and red signals in DNA FISH and RNA-DNA FISH experiments are shown. Sample type indicates whether samples came from single cell suspensions or tissue sections. Tissue indicates origin of the cells used for FISH. ZPA, intermediate, and anterior limb buds were excised from E10.5 embryos. The posterior third of limb buds were also isolated from E12.5 embryos. Δ MFCS1 limb buds were excised from the posterior region of E10.5 Δ MFCS1 embryos.

As limb development progresses, *Shh* expression is quickly downregulated and becomes undetectable by E12.5. Therefore, we examined temporal changes in the physical distance between MFCS1 and the *Shh* coding region during the course of limb development. Since descendants of *Shh*-expressing cells are distributed more widely in the posterior limb buds at E12.5 (Harfe et al., 2004), 3D-FISH analysis was carried out using the posterior third of forelimbs at E12.5. When compared to E10.5 embryos, the frequency of colocalized signals (6%) was significantly reduced ($p < 0.01$, chi-square test), whereas the frequencies of separated signals were elevated ($p < 0.01$, Kolmogorov-Smirnov test; Figure 2G).

To examine whether the long-range MFCS1-*Shh* interaction is specific to the *Shh* locus, we investigated distance changes in another probe pair with the same genomic distance as in the case of MFCS1 and *Shh*. Two BAC DNA clones, RP24-335O17 (approximately 100 kb upstream of *Lmbr1*) and RP23-446J15 (in a genomic region including *Otof*) were used as probes (see Figure S1 available online). In ZPA cells, the frequency of colocalized signals for the control probe pair was far less than that for the probes for *Shh* and MFCS1 ($p < 0.01$, chi-square test; Figure S1). The two signals for the control probe pair was mostly separated by 0.4 to 1.2 μ m, contrasting with the frequency distribution of the MFCS1-*Shh* distance ($p < 0.01$, Kolmogorov-Smirnov test).

To determine whether a chromatin loop is formed around the *Shh* locus in ZPA cells, the topology of a middle point between MFCS1 and the *Shh* coding region was examined. Fosmid DNA containing the telencephalic *Shh* enhancer SBE4 (Jeong et al., 2006), which is approximately 340 kb upstream from the *Shh* coding region, was used as a probe for the intervening segment (Figure 1A). The SBE4 signal was usually separate from either the MFCS1 or the *Shh* signal in ZPA cells. The frequency of

colocalization of the SBE4 signal with the *Shh* and MFCS1 signals was significantly lower than that of colocalization between MFCS1 and *Shh* signals ($p < 0.01$ for both, chi-square test; Figures 2H and 2I, respectively). The overall frequency distributions of the SBE4-*Shh* and MFCS1-SBE4 distance were significantly different from that of the MFCS1-*Shh* distance ($p < 0.01$ for both, Kolmogorov-Smirnov test). This suggests that SBE4 is not involved in the close physical association between MFCS1 and the *Shh* locus. On the contrary, enhancer-promoter interactions in this context seem quite specific and do not reflect a gross chromatin condensation around the *Shh* locus.

Chromosome Conformation Capture Assay Reveals an Interaction between MFCS1 and the *Shh* TSS

To confirm the physical interaction between MFCS1 and the *Shh* coding region, we used the chromosome conformation capture (3C) method, which has been used to measure associations between two genomic regions, such as LCRs and promoters (Dekker et al., 2002). *Shh*-expressing limb buds and forebrains in E10.5 embryos, as well as the distal tip of tail buds and E12.5 limb buds, which do not express *Shh*, were isolated. Crosslinked genomic DNA in prepared cells were digested with HindIII and then ligated. PCR primers were designed to each HindIII fragment to detect unique ligation products. Besides primers for sequences containing the putative *Shh* TSS and MFCS1, we used other primers for SBE4, *Lmbr1* promoter, and a fragment 260 kb upstream of the *Shh* TSS as controls (Figure 3A). We quantified the degree of interaction of the *Shh* TSS with other four regions by real-time PCR. In the limb bud, specific interactions between MFCS1 and the *Shh* TSS were detected at E10.5, but not at E12.5. MFCS1-*Shh* TSS interactions were reduced in the forebrain and tail bud, and no significant interactions were observed between the *Shh* TSS and other intervening segments (Figure 3B). Consistent with the 3D-FISH results, these data indicate that MFCS1 interacts directly with the *Shh* TSS in the limb bud.

Transcriptional Activity at the *Shh* Locus Correlates with Chromosome Conformation

To determine whether the proximity of MFCS1 and the *Shh* TSS is coupled with *Shh* transcriptional activity, the physical distance between MFCS1 and *Shh* pre-mRNA, which marks the *Shh* transcriptional initiation site, was analyzed by RNA-DNA double FISH. Sections of mouse E10.5 embryos were hybridized with probes for the first and the second introns of *Shh* to detect the pre-mRNA. Signal for *Shh* pre-mRNA was detected in posterior but not in anterior limb bud cells (Figure S2). To confirm that the pre-mRNA signal represents transcription from the *Shh* locus, the sections were hybridized with probes for the *Shh* pre-mRNA and the *Shh* coding region. In the *Shh*-expressing ZPA cells, 58% of the pre-mRNA signal colocalized with the *Shh* coding region signal, and 38% of the pre-mRNA signal was closely located within 0.2–0.4 μ m of the *Shh* coding region signal (Figures 4A and 4B).

Next, we measured the distance between MFCS1 and the *Shh* pre-mRNA. As a negative control for a nonenhancer element, genomic DNA from the BAC clone RP24-374O23, which is located 1 Mb downstream of the *Shh* coding region in the opposite direction to MFCS1 was used (Figure 1A). Forty-eight percent of *Shh*

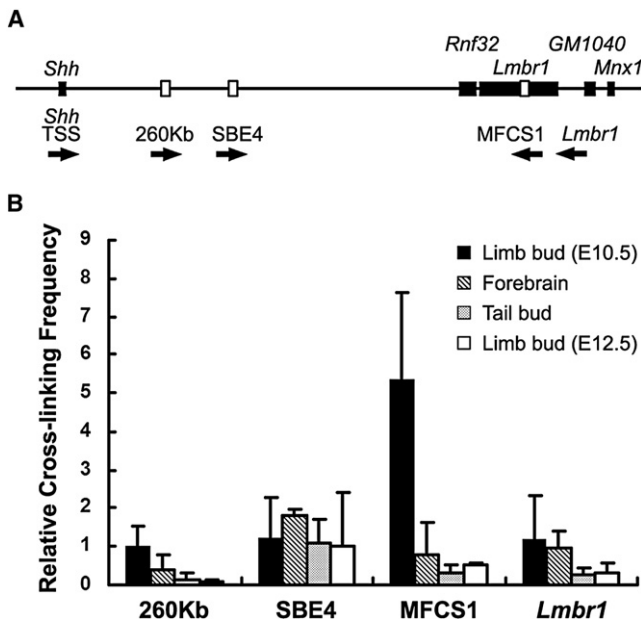


Figure 3. 3C Assay Reveals Physical Interactions between MFCS1 and the *Shh* TSS

(A) Map of target genomic regions for the 3C assay. Arrows under the diagram of the *Shh* locus show primers designed to the ends of the HindIII fragments. (B) Relative frequencies of cross-linking between the *Shh* TSS and the ends of other selected HindIII fragments in E10.5 limb buds (black bars), E10.5 forebrain (shaded bars), E10.5 tail bud (dotted bars), and E12.5 limb bud (open bars). Crosslinking frequencies are shown as the mean values from real-time PCR performed in triplicate and normalized using a primer pair for the β -actin promoter. The value of crosslinking frequency between the *Shh* TSS and the 260 Kb upstream region in E10.5 limb buds was set as 1. Error bars represent the standard deviations (SD) obtained from three independent experiments.

pre-mRNA signal was colocalized with the MFCS1 signal, and 36% of *Shh* pre-mRNA signal was within 0.2–0.4 μ m of the MFCS1 signal in ZPA cells (Figures 4C and 4D). The overall distance frequency distribution was similar to that observed in the RNA-DNA double FISH with probes for the pre-mRNA and for the *Shh* coding region ($p = 0.382$, Kolmogorov-Smirnov test). In contrast, signal for the control BAC DNA was far from the *Shh* pre-mRNA signal ($p < 0.01$, Kolmogorov-Smirnov test; Figures 4E and 4F). The frequency of colocalization of the MFCS1 and *Shh* pre-mRNA signals was much higher than that of the signals for MFCS1 and the *Shh* coding region, which was estimated by DNA FISH ($p < 0.01$, chi-square test; Figures 2D and 4D). These data indicate that chromosomal conformation at the *Shh* locus is correlated with transcriptional activity.

MFCS1 Interacts with the *Shh* Coding Region, but the *Shh* Locus Remains in its Chromosome Territory in MFCS1 Deletion Mutants

Deletion of MFCS1 from the mouse genome causes a dramatic reduction in the expression level of *Shh* in the limb bud (Sagai et al., 2005). To test whether MFCS1 is itself involved in the dynamic changes in chromosome conformation, we examined the physical interaction between the *Shh* coding region and the genomic region near MFCS1 in the limb buds of Δ MFCS1 homo-

zygous mutant embryos. Sections of Δ MFCS1 embryos and wild-type littermates at E10.5 were hybridized with labeled *Shh* and MFCS1 probes to measure the distance between the two signals in ZPA nuclei (Figures 5A and 5B). Although the frequency of colocalized signals ($<0.2 \mu$ m) in sectioned posterior limb buds of Δ MFCS1 embryos was somewhat lower than that observed in isolated cell preparations, it is comparable to that of their sectioned wild-type littermates ($p = 0.662$, chi-square test; Figure 5C). This suggests that MFCS1 is not required for the interaction to occur at the *Shh* locus.

Even though *Shh* is not expressed in the anterior limb bud of wild-type embryos and the posterior limb bud of Δ MFCS1 embryos, signals of MFCS1 and *Shh* coding region were colocalized in cells of the above tissues. These data suggest that MFCS1 sequence does not control long-range physical interactions nor the transcriptional competence that appears to accompany them. Rather, the ability of this region to interact with the *Shh* TSS must be controlled by other determinants, while MFCS1 itself would appear to be involved in frank transcriptional activation of *Shh* expression. To elucidate the difference in chromosome conformation between *Shh*-expressing and nonexpressing cells, further 3D-DNA FISH analyses were carried out, this time focusing on the topology of the *Shh* locus relative to the territory of chromosome 5 to which *Shh* maps. The frequency distribution of distance between the *Shh* locus and the CT surface is shown in Figure 5G. The distance divided by the diameter of *Shh* signal was used for determining whether *Shh* signals were outside the CT. If the value was greater than 0.5, the *Shh* locus was judged to be looped out of the CT, as was previously reported (Scheuermann et al., 2004). Approximately 17% of *Shh* signal was outside the CT in the ZPA, ranging between 0.3 and 1.0 μ m from the CT surface (Figures 5D and 5G). The remaining signals were located around the territory surface rather than near the center of the CT. In the anterior limb bud and the posterior limb bud of Δ MFCS1 embryos, most of *Shh* signals were located around the territory surface without being away from the CT (Figures 5E and 5F). The Fisher's exact test revealed that the proportion of *Shh* signal outside the CT in the ZPA was significantly larger than that in the anterior limb bud and in the posterior limb bud of Δ MFCS1 embryos ($p < 0.01$ for both). Thus, while the general distribution of the *Shh* locus was similar in wild-type and mutant backgrounds, occasional looping out was seen under conditions in which *Shh* transcription occurred, i.e., in wild-type but not MFCS1 mutant cells. It would therefore appear that MFCS1 is required for looping out and for *Shh* transcription per se, even in the presence of long-range enhancer-promoter interactions.

Low Level, Punctate *Shh* Transcription Patterns in the ZPA

We have shown that MFCS1 and the *Shh* coding region colocalize in only a fraction of ZPA cells (Figure 2D), and only a proportion of ZPA cells are actively transcribing *Shh* pre-mRNA (Figure S2). Since *Shh* is generally thought to be expressed throughout the ZPA, it seems unlikely that our results identify a particular cell subpopulation. Thus, we prefer the hypothesis that *Shh* transcription fluctuates within an individual cell in the ZPA, depending upon the changing chromosome conformation. To examine this possibility further, we analyzed the distribution

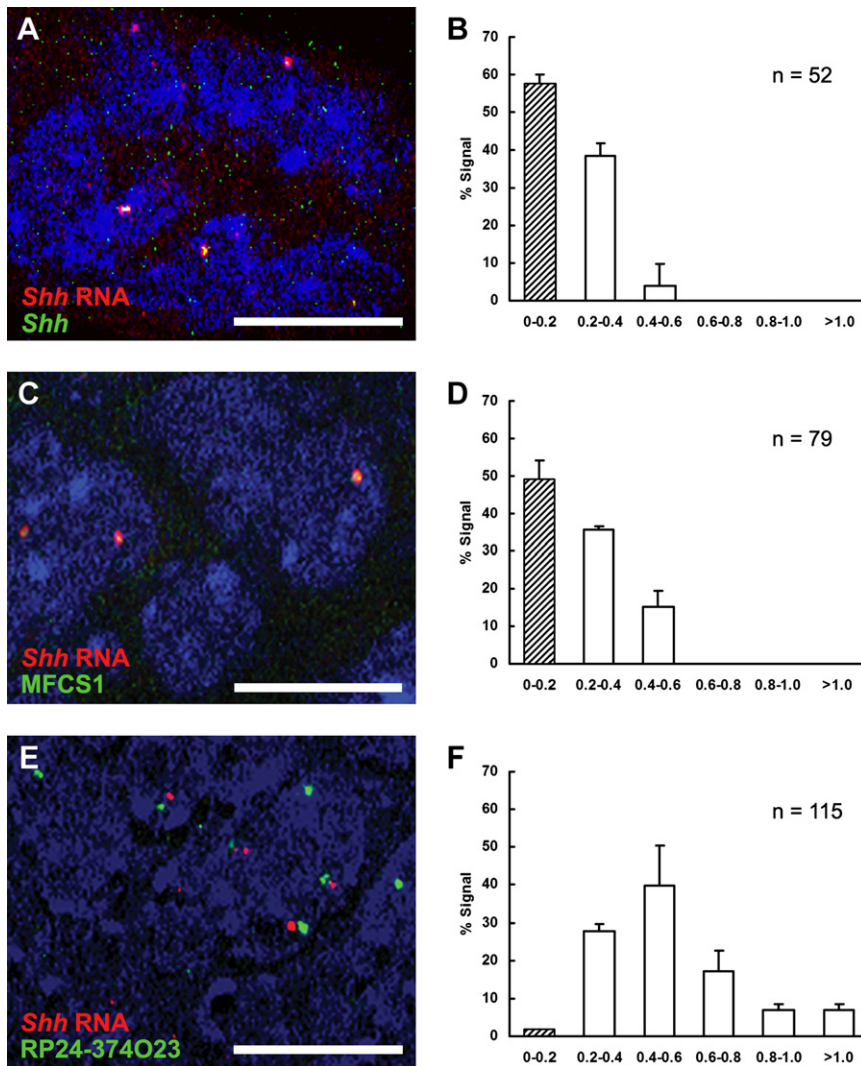


Figure 4. Physical Distance between MFCS1 and *Shh* Pre-mRNA

(A, C, and E) Magnified views of sections of the ZPA region hybridized with *Shh* intronic probes (red) and DNA probes (green) for the *Shh* coding region (A), MFCS1 (C), or the control region (E). Nuclei were stained blue with TOPRO-3. White bars, 10 μm.

(B, D, and F) Frequency distributions of the distance between the signals for *Shh* pre-mRNA and the *Shh* coding region (B), MFCS1 (D), or a control region (F). Shaded columns indicate fractions of colocalized signals (0–0.2 μm). Number (n) of loci observed in this experiment is shown. Error bars represent the standard deviations (SD) obtained from two independent experiments.

tion is different in the ZPA than in other *Shh*-expressing tissues; it appears to be weaker and more transient. These results are consistent with a model in which *Shh* transcription fluctuates dynamically within each cell of the ZPA.

DISCUSSION

The *Shh* Locus Has Three Different Chromosome Conformation States

Our data showed that the physical distance between MFCS1 and the *Shh* coding region changes along the anteroposterior axis of developing mouse limb buds. 3C- and 3D-FISH with a probe for the middle position in the MFCS1-*Shh* interval suggested that the physical interaction between enhancer and promoter is specific and does not reflect a gross condensation of the surrounding chromosomal DNA.

Unexpectedly, the interaction between MFCS1 and the *Shh* coding region was observed in the anterior limb buds, where *Shh* expression is not observed under normal conditions. The anterior limb bud margin is known to have the potential to express *Shh*, since ectopic *Shh* expression is observed in preaxial polydactylous mouse mutants and in the chick wing bud with retinoic acid-induced duplicated digits (Tickle et al., 1982; Masuya et al., 1997). Thus, the observed interaction of MFCS1 and the *Shh* coding region in the anterior limb bud cells likely indicates the competence of these cells to express *Shh*.

We also showed that the long-range MFCS1-*Shh* interaction is stage specific. The interaction disappears in the posterior limb bud cells at E12.5 (Figure 2G), as endogenous *Shh* expression ceases. However, it was previously shown that MFCS1 can drive *LacZ* reporter in the limb buds of E13.5 embryos when juxtaposed with a functional promoter (Lettice et al., 2003). Since *Hoxd* and *Fgf* genes encode upstream factors involved in *Shh* activation and still remain active at this stage (Dollé et al., 1989; Zakany et al., 2004; Sun et al., 2002), it is likely that MFCS1 can act as an enhancer when juxtaposed to an appropriate promoter at later developmental stages. Our data suggest

pattern of *Shh* pre-mRNA and mRNA on the same sections of E10.5 mouse embryos. In the limb bud, *Shh* mRNA was uniformly expressed in a group of mesenchymal cells beneath the ectoderm (Figure 6A), whereas *Shh* pre-mRNA was observed only in 37% of the mRNA-positive cells (Figure 6B; Table 2). As a control, we also examined the ratio of *Shh* pre-mRNA-positive cells to *Shh* mRNA-positive cells, in the notochord and floor plate. The strong expression of *Shh* in these central nervous system tissues is mediated by both intronic and 5' (8 kb upstream of the *Shh* TSS) enhancers (Epstein et al., 1999). We found that 68% of *Shh* mRNA-positive cells in the notochord and floor plate are also positive for *Shh* pre-mRNA (Figures 6C and 6D; Table 2). Finally, we generated a *d2EGFP* knock-in mouse in which a cassette expressing an unstable, transient GFP variant was inserted into the *Shh* locus (Figure S3). Immunohistochemical analysis of this knockin mouse embryo revealed punctate *d2EGFP* expression in cells scattered within the ZPA (Figure 6E). In contrast, almost all notochord and floor plate cells expressed *d2EGFP* (Figure 6F). Moreover, the intensity of *d2EGFP* expression in the ZPA was far lower than in the floor plate and notochord. Collectively, these data suggest that the activation of *Shh* transcrip-

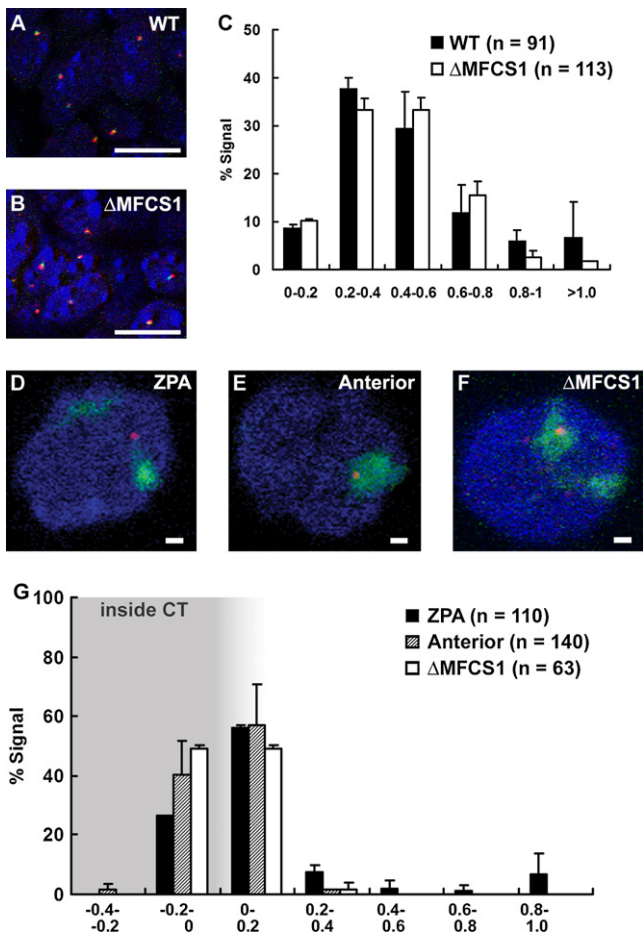


Figure 5. The *Shh* Locus Loops Out from Its Chromosome Territory in ZPA Cells

(A and B) DNA FISH using probes for the *Shh* coding region and MFCS1 in the ZPA region of sectioned wild-type (A) and Δ MFCS1 (B) embryos. Nuclei were stained with TOPRO-3 (blue). White bars, 10 μ m.

(C) Frequency distributions of the distances between two signals shown in A (black bars) and B (open bars). Error bars represent the standard deviations (SD) obtained from two independent experiments. Number (n) of loci observed in this experiment is shown.

(D–F) 3D-FISH was carried out for ZPA cells (D), anterior bud cells (E), and posterior bud cells (F) of Δ MFCS1 embryos using probes for mouse chromosome 5 territory (green) and the *Shh* coding region (red). Nuclei were stained with TOPRO-3 (blue). White bars, 1 μ m.

(G) Frequency distributions of the distance between signals for the *Shh* coding region and the CT surface in ZPA cells (black bars), anterior bud cells (shaded bars), and posterior bud cells (open bars) of Δ MFCS1 embryos. Error bars represent the standard deviations (SD) obtained from two independent experiments.

that competence to express *Shh* is primarily due to long-range enhancer-promoter interactions, but that the MFCS1 sequence itself is required for subsequent steps, associated with looping out and transcriptional activation (see below).

Gene loci under active transcription often loop out from their CT (Volpi et al., 2000; Mahy et al., 2002a; Williams et al., 2002; Chambeyron and Bickmore, 2004; Brown et al., 2006). In some cases, active genes located away from the CT colocalize with focal concentrations of RNA polymerase II known as transcription

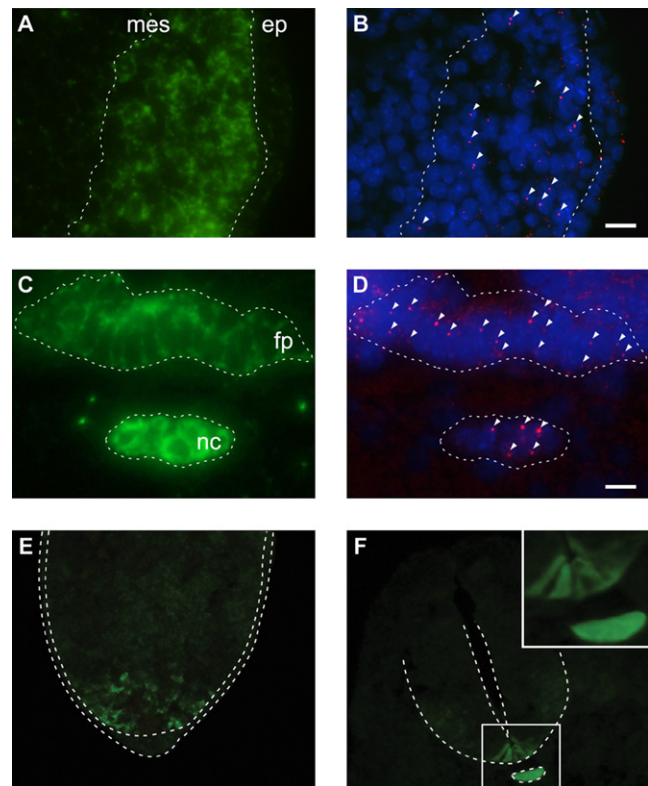


Figure 6. Expression of d2EGFP in the ZPA of *d2EGFP* Knockin Mouse

(A–D) RNA double FISH of 4 μ m sections of the ZPA (A and B) and the central nervous tissues (C and D) of E10.5 embryos. The sections were simultaneously hybridized with the *Shh* mRNA probe (green; A and C) and the intronic probes (red; B and D). Dashed lines and white arrowheads represent contours of the mRNA-positive regions and the pre-mRNA signals, respectively. me, mesenchyme; ep, epithelium; fp, floor plate; nc, notochord. White bars in (B) and (D), 10 μ m.

(E and F) Expression pattern of d2EGFP in the limb bud (E) and the neural tube (F) of the *d2EGFP* knockin mouse at E10.5. Dashed lines represent contours of the limb bud, neural tube, and notochord. Inset in (F) is a magnified view of the floor plate and notochord.

factories, suggesting that such genes loop out from the CT to share the same factory (Osborne et al., 2004). However, genes that are undergoing active transcription do not necessarily relocate outside their CTs (Abranches et al., 1998; Verschure et al., 1999; Mahy et al., 2002b; Sadoni and Zink, 2004; Morey et al., 2007). Therefore, involvement of gene relocation relative to the CT seems to be specific to each gene locus. This study showed the *Shh* locus relocates outside of the CT in wild-type cells of the ZPA, but not in anterior limb bud cells or posterior limb bud cells of the Δ MFCS1 mutant. Thus, MFCS1 function correlates with looping out and with active *Shh* transcription in limb buds.

We further demonstrated that deletion of MFCS1 from the mouse genome does not influence MFCS1-*Shh* interaction but does significantly affect looping out of the *Shh* locus from the CT (Figure 5). This result is consistent with a report showing that the mutant β -globin allele lacking the locus control region mostly stays in the CT in human erythroid cells (Ragoczy et al., 2003). Given that the *Shh* locus remains in anterior

Table 2. Proportion of *Shh* pre-mRNA-Positive Cells among mRNA-Positive Cells

Tissue	No. of pre-mRNA-Positive Cells	Total No. of Cells	Mean% \pm SD
ZPA	207	562	37.04 \pm 1.40
Nc, Fp	141	207	68.10 \pm 1.99*

The number of pre-mRNA-positive cells was counted in *Shh* mRNA-positive cells in the ZPA, notochord (Nc), and floor plate (Fp). Five or six independent sections were used for the counting. Total Cells represents the total number of *Shh* mRNA-positive cells in the ZPA and each tissue. The difference in the proportion of *Shh* pre-mRNA-positive cells between the ZPA and the central nervous tissues is statistically highly significant by the chi-square test (* $p < 0.001$).

limb bud cells (Figure 5), it is likely that the MFCS1-*Shh* interaction and looping out from the CT are independent events. It is unknown, however, if these two events occur sequentially, but our data favor a model in which the MFCS1-*Shh* interaction precedes the looping out, because we observed MFCS1-*Shh* interaction without looping out in both the posterior limb buds of Δ MFCS1 embryos and the anterior limb buds of wild-type embryos, whereas looping out in the absence of the MFCS1-*Shh* interaction has not been observed so far.

Based on our results, we propose a model in which limb bud cells have three different chromosome conformation states in relation to *Shh* expression. In the silent state, MFCS1 is far from the *Shh* coding region, as is the case in the intermediate portion of the limb bud, where ectopic *Shh* expression is never observed. In the poised state, MFCS1 interacts with the *Shh* coding region, but the interacting regions stay within the CT, as is observed in anterior limb bud cells. Finally, in the active state, the MFCS1 interacts with the *Shh* coding region and the *Shh* locus relocates outside the CT. This state is specific to the ZPA cells, in which *Shh* is actively expressed.

Mosaic Transcriptional Activation of *Shh* in ZPA Cells

The most striking finding in this study is that individual cells in the ZPA have different chromosome conformations. Long-range enhancer-promoter interactions at the *Shh* locus occur only in a small fraction (18%) of chromosomes in ZPA cells (Figure 2D) and almost the same proportion of alleles shows looping out from the CT (Figure 5G). Given that *Shh* mRNA is detectable in every ZPA cell (Figure 6A), it is most likely that a pulse of *Shh* transcription occurs in each ZPA cell rather than in a restricted fraction of ZPA cells. Thus, it is possible that the chromosome conformation around the *Shh* locus shows dynamic transitions between the silent, poised, and active states in ZPA cells.

We also showed that the *Shh* pre-mRNA colocalizes with the *Shh* coding region by RNA-DNA double FISH (Figure 4B), as was previously reported for other loci under active gene expression (Wilkie et al., 1999; Shav-Tal et al., 2004). In addition, 48% of the *Shh* pre-mRNA signal is colocalized with the MFCS1 signal (Figure 4D). These data show that the physical interaction between MFCS1 and the *Shh* coding region is well correlated with the transcriptional activity of the *Shh* locus. However, we observed that 37% of ZPA cells are positive for *Shh* pre-mRNA signal (Figure 6B), while about 65% of alleles in these pre-

mRNA positive cells are actually producing *Shh* pre-mRNA, based on the RNA FISH, examining mono- and biallelic expression of *Shh* pre-mRNA in ZPA cells (Figure S2). Thus, about 24% of the alleles in ZPA cells appear to actually express *Shh* pre-mRNA at any given time. Since 48% of the *Shh* pre-mRNA signal was colocalized with the MFCS1 signal, at most 12% of the alleles should show MFCS1-*Shh* pre-mRNA colocalization. However, we instead observed that 18% of alleles in ZPA cells show MFCS1-*Shh* interaction (Figure 2D). The reason for this discrepancy is not clear at present. One possibility is that the MFCS1-*Shh* interaction occurs even in the pre-mRNA negative ZPA cells, as is the case in the anterior limb bud cells. Alternatively, the discrepancy may be due to differences in efficiency of signal detection between RNA and DNA FISH analysis.

Short- and Long-Range Enhancers Regulate Different Modes of *Shh* Expression in Different Tissues

We found that more cells in the floor plate and notochord are actively transcribing *Shh* pre-mRNA at any given time than cells in the ZPA. Since GFP reporter expression was previously shown to be present in almost all ZPA cells in *Shh-Gfpcre* mice in which a stable GFP was inserted at the *Shh* locus (Harfe et al., 2004), it is likely that this mosaicism reflects temporal fluctuations in *Shh* transcription within individual cells rather than the existence of a restricted population of *Shh*-expressing cells. This was confirmed by our analysis of *d2EGFP* knockin mice, which were made in the same way as the *Shh-Gfpcre* reporter mice but instead express an unstable, transient *d2EGFP* protein under the control of the *Shh* locus. *d2EGFP* is more strongly and widely expressed in the floor plate and notochord than in the ZPA, which showed punctate, scattered expression, likely due to an insufficient accumulation of *d2EGFP* in many ZPA cells.

Taken together, our data indicate that the different modes of *Shh* expression between neural tissues and the limb bud ZPA are correlated with the usage of the two different types of enhancers. In neural tissues, the strong and long-lasting expression of *Shh* is regulated by short-range enhancers. In contrast, a long-range enhancer is used in the ZPA, where *Shh* is expressed at a lower level and for a shorter duration. In particular, an abrupt initiation of *Shh* expression at E9.5 and termination of expression at E12.5 is unique to the ZPA.

Transitioning between the three chromosome conformation states that reflect engagement of the MFCS1 enhancer with the *Shh* promoter and looping out of the *Shh* locus may be involved in the change of the *Shh* transcription during normal limb bud development. Since precise *Shh* protein concentration gradients are essential for normal morphogenesis in different tissues, it is likely that the appropriate long- and short-range enhancers are selectively used to control the precise concentration and spatiotemporal patterns of *Shh* expression.

EXPERIMENTAL PROCEDURES

Mice

C57BL/6J mice were purchased from Japan Clea Ltd. (Tokyo, Japan) and maintained at The National Institute of Genetics (NIG). C57BL/6J mouse embryos were used for 3D-FISH and 3C experiments. To produce a *d2EGFP* knock-in mouse, pKO Scrambler V901 (Lexicon Genetics Inc.) containing *neomycin* and *diphtheria toxin* cassettes was used to make the targeting vector. Gene targeting was carried out as described for the *Shh-Gfpcre* knockin

mouse (Harfe et al., 2004). Briefly, six nucleotides just prior to the *Shh* ATG were changed from 5'-GACGAG-3' to an XbaI site in a 1.2 kb of short homology arm. The *d2EGFP* cassette (Clontech) was connected to the short arm at the XbaI site. The first 35 bp nucleotides, including the *Shh* ATG, were eliminated from a 5' long homology arm (8.0 kb) so that the endogenous *Shh* allele becomes a null allele. In the knock-in mouse genome, the first 35 bp of the *Shh* gene was replaced by the *d2EGFP* cassette.

Real-Time PCR Analysis

Total RNA was isolated using the QIAeasy RNA isolation kit (QIAGEN) from both forelimb buds of each E10.5 embryo generated by an intercross of Δ MFCS1 heterozygotes. Individual embryos were genotyped as previously described (Sagai et al., 2005). First strand cDNA was synthesized from 500 ng total RNA with SuperScript III Reverse Transcriptase (Invitrogen). Quantitative real-time PCR analysis was performed on a 7700 Real-time PCR system (Applied Biosystems) using the Platinum SYBR Green qPCR SuperMix UDG kit (Invitrogen). Standard curves were generated by serial dilution of plasmids. All experiments were independently carried out in triplicate. Sequences of the oligonucleotide primers used are shown in Table S1.

DNA FISH

Approximately 20 kb genomic fragments containing the *Shh* coding region (BAC clone RP24-162A4) and MFCS1 (BAC clone RP24-265M10) were cloned into the Charomid vector (Nippongene). The Charomid DNA and RP24-374O23 were labeled with digoxigenin-11-dUTP (Roche) or DNP-11-dUTP (Perkin Elmer) using nick translation. To label mouse chromosome 5 in embryonic cell nuclei, we used mouse chromosome 5 painting probes prepared from flow-sorted chromosome 5, which was kindly provided by Dr. Michael Speicher (Jentsch et al., 2003). Probe labeling was performed by DOP-PCR (Telenius et al., 1992) in the presence of DNP-11-dUTP (Perkin Elmer). About 150 ng of probe and 7 μ g of mouse cot-1 DNA were used for hybridization. Fluorescent in situ hybridization was carried out as previously described (Solvei et al., 2002a, 2002b; Tanabe et al., 2002). Briefly, a small portion of target tissue was taken from mouse limb buds using a fine-sharpened tungsten needle. The tissue was suspended in 10% FCS/DMEM and passed through a thin glass capillary several times to obtain a single cell suspension. The cells were incubated at 37°C for 30 min on poly-L-lysine coated slides, and then were fixed with 4% PFA at room temperature for 10 min. For permeabilization, cells were treated with 0.5% saponin and 0.5% Triton X-100 for 20 min and then were incubated in 20% glycerol/PBS for at least 30 min, followed by five freeze-thaw cycles in liquid nitrogen. After treatment with 0.002% pepsin in 0.01 N HCl at 37°C for 1 min, cells were postfixed with 1% PFA for 10 min. Slides were stored in 50% formamide/2 \times SSC before hybridization. Predenatured probes were applied to the slides. The cells were denatured at 74°C for 4 min, and hybridization was performed at 37°C for 60 hr. Cells were then washed three times in 0.1 \times SSC at 60°C for 5 min each and blocked with 5% BSA in 4 \times SSC with 0.2% Tween-20. Anti-Dinitrophenyl (DNP) (Sigma) and Alexa Fluor 488 donkey anti-goat IgG (Invitrogen) were diluted to 1:200 and used to detect DNP-labeled probes. Monoclonal anti-Digoxigenin (Sigma) and Cy3-conjugated anti-mouse IgG (Jackson ImmunoResearch Inc.) were diluted to 1:300 and used to detect DIG-labeled probes. In our experiment, bi-allelic FISH signals were observed in 80% of nuclei.

3D Image Analysis

All images were obtained using confocal fluorescence microscopy (LSM510 META). Chromosome territories and BAC clone FISH signals were recorded in three separate RGB channels. The image stacks were 3D-reconstructed using a program developed for chromosome territory measurement (AVS/Express Developer Version 7.0; KGT Co., Ltd). The reasonable thresholds for each channel were determined by a whole 3D coordination of the volume of gene signals. The shortest distance between the gravity centers of the gene-to-gene or the distance between the gravity centers of the gene and the surface of its chromosome territory was calculated.

Statistical Analysis

Two-tailed Welch's *t* test was used to test significance of differences in gene expression level (Figure 1). Kolmogorov-Smirnov test was used to test significance of difference in frequency distribution of distance of two FISH signals

(Figure 2). Chi-square test was used to test significance of difference in frequency of colocalized signals (Figures 2 and 4), and proportion of pre-mRNA positive cells in mRNA positive cells (Figure 6). Fisher's exact test was used to test significance of difference in proportion of looped out signals (Figure 5). The latter three tests are used without assuming that observations have normal distribution. Kolmogorov-Smirnov test and Fisher's exact test were performed using the computing software R (<http://www.r-project.org>).

3C Assay

The 3C assay was performed as previously reported (Dekker et al., 2002; Osborne et al., 2004). Briefly, embryonic tissues were subjected to 0.125% Trypsin and 0.5 mM EDTA in PBS at 37°C for 10 min and then dissociated into a single cell suspension in 10% FCS/DMEM by gentle pipetting. 1×10^6 cells were crosslinked with 2% formaldehyde for 10 min at room temperature. After cell lysis, DNA was digested with HindIII overnight at 37°C. Digested chromatin was treated with 30 Weiss units of T4 DNA ligase at 16°C for 4 hr. After protein digestion and reverse cross-linking, samples were subjected to real-time PCR. To prepare positive control templates, we used BAC clones containing all regions of interest. RP24-162A4 (the putative *Shh* TSS), RP24-352G17 (the 260 kb upstream region of the *Shh* TSS and SBE4) and RP24-265M10 (MFCS1 and the putative *Lmbr1* TSS) were used. Equimolar amounts of different two BAC DNA samples were mixed, digested with HindIII, and then ligated. We used the control templates to draw standard curves for the quantitative real-time PCR, which was performed as described above. PCR products were isolated from gels and sequenced to confirm formation of chimeric fragments. Sequences of the oligonucleotide primers used are shown in Table S1.

RNA-DNA FISH

DNA probes were synthesized using a Charomid-*Shh* and a BAC clone, RP24-374O23, as templates. Introns 1 and 2 of *Shh* were individually cloned into a vector for synthesis of antisense riboprobe. The plasmid were digested with NotI and SpeI and then transcribed with DIG RNA labeling mix (Roche) by T3 and T7 RNA polymerase, respectively. The fragment size of the DIG-labeled riboprobes was reduced to 1000 bp or smaller by alkaline hydrolysis. Hybridization was carried out with minor revisions of the standard protocol. Briefly, 4 μ m paraffin sections of mouse embryos were mounted on MAS-coated slides and deparaffinized by washing four times in xylene. After washing once in ethanol, they were treated in ethanol containing 1% hydrogen peroxide for 30 min. Then, the sections were rehydrated through an ethanol series, treated with 1 μ g/ml Proteinase K, and fixed with 4% paraformaldehyde. After dehydration through an ethanol series and air-drying, the sections were hybridized with the riboprobes overnight at 65°C. Monoclonal anti-Digoxigenin (Sigma) and Cy3-conjugated anti-mouse IgG were used as primary and secondary antibodies. Antibodies were fixed with 4% PFA for 10 min before DNA hybridization. Subsequent DNA FISH was carried out as reported previously (Chambeyron et al., 2005). Briefly, the sections were denatured in 70% formamide/2 \times SSC at 75°C for 3 min and then passed through ice-cold 70% ethanol. After dehydration through an ethanol series and air-drying, the sections were hybridized with DNA probes. The subsequent steps were same as described for DNA FISH on cell suspensions.

Pre-mRNA/mRNA Double In Situ Hybridization

The same DIG-labeled riboprobes were used for *Shh* Pre-mRNA and RNA-DNA FISH. A FITC-labeled riboprobe for *Shh* mRNA was transcribed with FITC RNA labeling mix (Roche) using a *Shh* plasmid clone, as reported previously (Sagai et al., 2005). Pre-mRNA was detected as described for RNA-DNA FISH. We detected the FITC-labeled probe by using TSA Plus Fluorescence Systems (PerkinElmer Co., Ltd), according to the manufacturer's protocol. Briefly, pre-mRNA-detected sections were blocked in TNB buffer for 30 min, and then incubated with Anti-Fluorescein-POD Fab fragments (Roche) diluted to 1:100 in TNB buffer for 1 hr. After being washed in TNT buffer, sections were incubated with Fluorescein-labeled Tyramide for 20 min. Nuclei were stained with 1 μ g/ml of DAPI in TBST.

Immunohistochemistry

Shh-d2EGFP knockin embryos were fixed in 4% paraformaldehyde for 1 hr, soaked in 30% sucrose and then embedded in OCT compound. Ten micrometer sections were blocked in 1% skim milk in PBS. Anti-GFP rabbit IgG

(Invitrogen) was diluted to 1:500 and the secondary antibody, HRP-conjugated anti-rabbit goat IgG (Jackson ImmunoResearch Laboratories, Inc.), was diluted to 1:200. Tyramide signal amplification was carried out by TSA Plus Fluorescence Systems according to the manufacturer's protocol (PerkinElmer Co., Ltd).

SUPPLEMENTAL DATA

Supplemental Data include three figures and one table and can be found with this article online at [http://www.developmentalcell.com/supplemental/S1534-5807\(08\)00485-1](http://www.developmentalcell.com/supplemental/S1534-5807(08)00485-1).

ACKNOWLEDGMENTS

We thank Michael R. Speicher (TU, Munich, Germany, presently Medical University, Graz, Austria) for providing the mouse chromosome 5 painting probe, Andrew P. McMahon for the *Shh* probe, and Hironori Fujisawa for statistical analyses. This study was supported in part by grants-in-aid from the Ministry of Education, Culture, Sports, Science and Technology of Japan. This study is contribution number 2512 from The National Institute of Genetics, Mishima, Japan.

Received: March 26, 2008

Revised: October 31, 2008

Accepted: November 18, 2008

Published online: December 18, 2008

REFERENCES

- Abranches, R., Beven, A.F., Aragón-Alcaide, L., and Shaw, P.J. (1998). Transcription sites are not correlated with chromosome territories in wheat nuclei. *J. Cell Biol.* *143*, 5–12.
- Brown, J.M., Leach, J., Reittie, J.E., Atzberger, A., Lee-Prudhoe, J., Wood, W.G., Higgs, D.R., Iborra, F.J., and Buckle, V.J. (2006). Coregulated human globin genes are frequently in spatial proximity when active. *J. Cell Biol.* *172*, 177–187.
- Capellini, T.D., Di Giacomo, G., Salsi, V., Brendolan, A., Ferretti, E., Srivastava, D., Zappavigna, V., and Selleri, L. (2006). Pbx1/Pbx2 requirement for distal limb patterning is mediated by the hierarchical control of Hox gene spatial distribution and *Shh* expression. *Development* *133*, 2263–2273.
- Carter, D., Chakalova, L., Osbourne, C.S., Dai, Y.F., and Fraser, P. (2002). Long-range chromatin regulatory interactions in vivo. *Nat. Genet.* *32*, 623–626.
- Chambeyron, S., and Bickmore, W.A. (2004). Chromatin decondensation and nuclear reorganization of the HoxB locus upon induction of transcription. *Genes Dev.* *18*, 1119–1130.
- Chambeyron, S., Da Silva, N.R., Lawson, K.A., and Bickmore, W.A. (2005). Nuclear re-organization of the Hoxb complex during mouse embryonic development. *Development* *132*, 2215–2223.
- Cremer, T., Cremer, M., Dietzel, S., Müller, S., Solovei, I., and Fakan, S. (2006). Chromosome territories—a functional nuclear landscape. *Curr. Opin. Cell Biol.* *18*, 307–316.
- Dekker, J., Rippe, K., Dekker, M., and Kleckner, N. (2002). Capturing chromosome conformation. *Science* *295*, 1306–1311.
- Dollé, P., Izpisua-Belmonte, J.C., Falkenstein, H., Renucci, A., and Duboule, D. (1989). Coordinate expression of the murine Hox-5 complex homeobox-containing genes during limb pattern formation. *Nature* *342*, 767–772.
- Epstein, D.J., McMahon, A.P., and Joyner, A.L. (1999). Regionalization of Sonic hedgehog transcription along the anteroposterior axis of the mouse central nervous system is regulated by Hnf3-dependent and -independent mechanisms. *Development* *126*, 281–292.
- Foster, H.A., and Bridger, J.M. (2005). The genome and the nucleus: a marriage made by evolution. *Genome organization and nuclear architecture. Chromosoma* *114*, 212–229.
- Fraser, P., and Bickmore, W. (2007). Nuclear organization of the genome and the potential for gene regulation. *Nature* *447*, 413–417.
- Harfe, B.D., Scherz, P.J., Nissim, S., Tian, H., McMahon, A.P., and Tabin, C.J. (2004). Evidence for an expansion-based temporal *Shh* gradient in specifying vertebrate digit identities. *Cell* *118*, 517–528.
- Jentsch, I., Geigl, J., Klein, C.A., and Speicher, M.R. (2003). Seven-fluorochrome mouse M-FISH for high-resolution analysis of interchromosomal rearrangements. *Cytogenet. Genome Res.* *103*, 84–88.
- Jeong, Y., El-Jaick, K., Roessler, E., Muenke, M., and Epstein, D.J. (2006). A functional screen for sonic hedgehog regulatory elements across a 1 Mb interval identifies long-range ventral forebrain enhancers. *Development* *133*, 761–772.
- Kleinjan, D.A., and van Heyningen, V. (2005). Long-range control of gene expression: emerging mechanisms and disruption in disease. *Am. J. Hum. Genet.* *76*, 8–32.
- Kmita, M., Tarchini, B., Zakany, J., Logan, M., Tabin, C.J., and Duboule, D. (2005). Early developmental arrest of mammalian limbs lacking HoxA/HoxD gene function. *Nature* *435*, 1113–1116.
- Knezevic, V., De Santo, R., Schughart, K., Huffstadt, U., Chiang, C., Mahon, K.A., and Mackem, S. (1997). Hoxd-12 differentially affects preaxial and postaxial chondrogenic branches in the limb and regulates Sonic hedgehog in a positive feedback loop. *Development* *124*, 4523–4536.
- Lañcôt, C., Cheutin, T., Cremer, M., Cavalli, G., and Cremer, T. (2007). Dynamic genome architecture in the nuclear space: regulation of gene expression in three dimensions. *Nat. Rev. Genet.* *8*, 104–115.
- Lettice, L.A., Heaney, S.J., Purdie, L.A., Li, L., de Beer, P., Oostra, B.A., Goode, D., Elgar, G., Hill, R.E., and de Graaff, E. (2003). A long-range *Shh* enhancer regulates expression in the developing limb and fin and is associated with preaxial polydactyly. *Hum. Mol. Genet.* *12*, 1725–1735.
- Li, Q., Barkess, G., and Qian, H. (2006). Chromatin looping and the probability of transcription. *Trends Genet.* *22*, 197–202.
- Ling, J.Q., Li, T., Hu, J.F., Vu, T.H., Chen, H.L., Qiu, X.W., Cherry, A.M., and Hoffman, A.R. (2006). CTCF mediates interchromosomal colocalization between *Igf2/H19* and *Wsb1/Nf1*. *Science* *312*, 269–272.
- Mahy, N.L., Perry, P.E., and Bickmore, W.A. (2002a). Gene density and transcription influence the localization of chromatin outside of chromosome territories detectable by FISH. *J. Cell Biol.* *159*, 753–763.
- Mahy, N.L., Perry, P.E., Gilchrist, S., Baldock, R.A., and Bickmore, W.A. (2002b). Spatial organization of active and inactive genes and noncoding DNA within chromosome territories. *J. Cell Biol.* *157*, 579–589.
- Masuya, H., Sagai, T., Moriwaki, K., and Shiroishi, T. (1997). Multigenic control of the localization of the zone of polarizing activity in limb morphogenesis in the mouse. *Dev. Biol.* *182*, 42–51.
- Masuya, H., Sezutsu, H., Sakuraba, Y., Sagai, T., Hosoya, M., Kaneda, H., Miura, I., Kobayashi, K., Sumiyama, K., Shimizu, A., et al. (2007). A series of ENU-induced single-base substitutions in a long-range cis-element altering Sonic hedgehog expression in the developing mouse limb bud. *Genomics* *89*, 207–214.
- McMahon, A.P., Ingham, P.W., and Tabin, C.J. (2003). Developmental roles and clinical significance of hedgehog signaling. *Curr. Top. Dev. Biol.* *53*, 1–114.
- Morey, C., Da Silva, N.R., Perry, P., and Bickmore, W.A. (2007). Nuclear reorganization and chromatin decondensation are conserved, but distinct, mechanisms linked to Hox gene activation. *Development* *134*, 909–919.
- Osborne, C.S., Chakalova, L., Brown, K.E., Carter, D., Horton, A., Debrand, E., Goyenechea, B., Mitchell, J.A., Lopes, S., Reik, W., et al. (2004). Active genes dynamically colocalize to shared sites of ongoing transcription. *Nat. Genet.* *36*, 1065–1071.
- Ragoczy, T., Telling, A., Sawado, T., Groudine, M., and Kosak, S.T. (2003). A genetic analysis of chromosome territory looping: Diverse roles for distal regulatory elements. *Chromosome Res.* *11*, 513–525.
- Riddle, R.D., Johnson, R.L., Laufer, E., and Tabin, C. (1993). Sonic hedgehog mediates the polarizing activity of the ZPA. *Cell* *75*, 1401–1416.
- Sadoni, N., and Zink, D. (2004). Nascent RNA synthesis in the context of chromatin architecture. *Chromosome Res.* *12*, 439–451.

- Sagai, T., Masuya, H., Tamura, M., Shimizu, K., Yada, Y., Wakana, S., Gondo, Y., Noda, T., and Shiroishi, T. (2004). Phylogenetic conservation of a limb-specific, cis-acting regulator of Sonic hedgehog (*Shh*). *Mamm. Genome* 15, 23–34.
- Sagai, T., Hosoya, M., Mizushima, Y., Tamura, M., and Shiroishi, T. (2005). Elimination of a long-range cis-regulatory module causes complete loss of limb-specific *Shh* expression and truncation of the mouse limb. *Development* 132, 797–803.
- Scheuermann, M.O., Tajbakhsh, J., Kurz, A., Saracoglu, K., Eils, R., and Lichter, P. (2004). Topology of genes and nontranscribed sequences in human interphase nuclei. *Exp. Cell Res.* 301, 266–279.
- Shav-Tal, Y., Darzacq, X., Shenoy, S.M., Fusco, D., Janicki, S.M., Spector, D.L., and Singer, R.H. (2004). Dynamics of single mRNPs in nuclei of living cells. *Science* 304, 1797–1800.
- Solovei, I., Cavallo, A., Schermelleh, L., Jaunin, F., Scasselati, C., Cmarko, D., Cremer, C., Fakan, S., and Cremer, T. (2002a). Spatial preservation of nuclear chromatin architecture during three-dimensional fluorescence in situ hybridization (3D-FISH). *Exp. Cell Res.* 276, 10–23.
- Solovei, I., Walter, J., Cremer, M., Habermann, F., Schermelleh, L., and Cremer, T. (2002b). FISH on three-dimensionally preserved nuclei. In *FISH: A Practical Approach*, B. Beatty, S. Mai, and J. Squire, eds. (Oxford: Oxford University Press), pp. 119–157.
- Spilianakis, C.G., Lalioti, M.D., Town, T., Lee, G.R., and Flavell, R.A. (2005). Interchromosomal associations between alternatively expressed loci. *Nature* 435, 637–645.
- Sun, X., Mariani, F.V., and Martin, G.R. (2002). Functions of FGF signalling from the apical ectodermal ridge in limb development. *Nature* 418, 501–508.
- Tanabe, H., Küpper, K., Ishida, T., Neusser, M., and Mizusawa, H. (2002). Evolutionary conservation of chromosome territory arrangements in cell nuclei from higher primates. *Proc. Natl. Acad. Sci. USA* 99, 4424–4429.
- Telenius, H., Pelmeur, A.H., Tunnacliffe, A., Carter, N.P., Behmel, A., Ferguson-Smith, M.A., Nordenskjöld, M., Pfragner, R., and Ponder, B.A. (1992). Cytogenetic analysis by chromosome painting using DOP-PCR amplified flow-sorted chromosomes. *Genes Chromosomes Cancer* 4, 257–263.
- Tickle, C. (1981). The number of polarizing region cells required to specify additional digits in the developing chick wing. *Nature* 289, 295–298.
- Tickle, C., Alberts, B., Wolpert, L., and Lee, J. (1982). Local application of retinoic acid to the limb bud mimics the action of the polarizing region. *Nature* 296, 564–566.
- Tolhuis, B., Palstra, R.J., Splinter, E., Grosveld, F., and de Laat, W. (2002). Looping and interaction between hypersensitive sites in the active β -globin locus. *Mol. Cell* 10, 1453–1465.
- Verschure, P.J., van Der Kraan, I., Manders, E.M., and van Driel, R. (1999). Spatial relationship between transcription sites and chromosome territories. *J. Cell Biol.* 147, 13–24.
- Volpi, E.V., Chevret, E., Jones, T., Vatcheva, R., Williamson, J., Beck, S., Campbell, R.D., Goldsworthy, M., Powis, S.H., Ragoussis, J., et al. (2000). Large-scale chromatin organization of the major histocompatibility complex and other regions of human chromosome 6 and its response to interferon in interphase nuclei. *J. Cell Sci.* 113, 1565–1576.
- West, A.G., and Fraser, P. (2005). Remote control of gene transcription. *Hum. Mol. Genet.* 14, R101–R111.
- Wilkie, G.S., Shermoen, A.W., O'Farrell, P.H., and Davis, I. (1999). Transcribed genes are localized according to chromosomal position within polarized *Drosophila* embryonic nuclei. *Curr. Biol.* 9, 1263–1266.
- Williams, R.R., Broad, S., Sheer, D., and Ragoussis, J. (2002). Subchromosomal positioning of the epidermal differentiation complex (EDC) in keratinocyte and lymphoblast interphase nuclei. *Exp. Cell Res.* 272, 163–175.
- Zakany, J., Kmita, M., and Duboule, D. (2004). A dual role for Hox genes in limb anterior-posterior asymmetry. *Science* 304, 1669–1672.